Available online at www.sciencedirect.com
SCIENCE DIRECT®
International Journal of Heat and Mass Transfer 47 (2004) 3517–3531
International Journal of HEAT and MASS TRANSFER
www.elsevier.com/locate/ijhmt

Permeability determination of a deep argillite in saturated and partially saturated conditions

F. Homand, A. Giraud *, S. Escoffier [1], A. Koriche, D. Hoxha

LAEGO-ENSG, BP 40, Vandoeuvre-lès-Nancy Cedex F-54501, France

Received 15 May 2003; received in revised form 5 January 2004
Available online 2 April 2004

Abstract

This paper deals with the methods of determination of permeability in saturated and partially saturated conditions for low permeable porous rocks such as argillites. The modified version of the pulse test proposed by Hsieh et al. [Int. J. Rock Mech. Min. Sci. Geomech. Abstr. 18 (1981) 245] has been used to characterize permeability in the saturated case. It enables the hydraulic diffusivity and then the intrinsic permeability and the specific storage coefficient to be characterized. In partially saturated conditions the method of saline solution to impose relative humidity and then capillary pressure has been used. The permeability in the partially saturated range can be deduced form measurements of transient weight loss and deformations of a sample submitted to a decrease of relative humidity in an hermetic chamber. In the two cases, pulse and drying tests, original experimental devices have been developed. The parameter-identification procedure based on the solution of corresponding inverse problems is presented. First approach explicit or semi-explicit solutions for the direct problems are used. It shows that the simplified linear approach is useful to obtain correct order of magnitude of unknowns parameters.

Keywords: Porous media; Partially saturated; Inverse problem; Parameter identification; Permeability; Pulse test; Drying test

1. Introduction

In underground radioactive waste isolation project the transport properties of the surrounding rock mass are of fundamental importance to ensure the security (short term) and the safety (long term) of the site. In short term (from the underground opening until the post-closure period), the rock behaviour (influenced by the excavation, the ground support...) must ensure the stability of the excavation for worker health and safety whereas in long term (after the post-closure period), the confinement performances of the site must meet the objective of waste isolation from the accessible environment. During both periods, rock performances (rock mass stability and confining capacities) are highly dependent on intrinsic permeability and specific storage.

In the ANDRA underground waste isolation project, due to the very low permeability of the argillite ($k \approx 10^{-20}$–10^{-22} m^2), the hydromechanical characterization in laboratory is limited. Below a certain permeability level, it becomes nearly impossible to conduct drained tests, to measure the pore fluid pressure or to control the saturation degree. Therefore the determination of its permeability is essential in order to master the experimental characterization of argillite coupled behaviour.

1.1. Saturated case

At the repository scale, although transmissive fractures could control the hydraulic behaviour of the surrounding clayey unit, Neuzil et al. [17] pointed out

* Corresponding author.
E-mail address: albert.giraud@ensg.inpl-nancy.fr (A. Giraud).
URL: http://www.laego.org.
[1] Present address: Division Reconnaissance et Mecanique des Sols (RMS), Laboratoire Central des Ponts et Chaussées (LCPC), Centre de Nantes, Route de Bouaye, BP 4129, F-44341 BOUGUENAIS Cedex.

0017-9310/$ - see front matter © 2004 Elsevier Ltd. All rights reserved.
doi:10.1016/j.ijheatmasstransfer.2004.02.012

Nomenclature

b	Biot coefficient (–)
$\boldsymbol{c}$	vector of unknown parameters (–)
C_{vp}	concentration of vapour (–)
C_{re}^{u}	upstream reservoir compressibility (pulse) (Pa/m^3)
C_{re}^{d}	downstream reservoir compressibility (pulse) (Pa/m^3)
D	liquid diffusivity (m^2/s)
h_r	relative humidity (–)
F	Fick coefficient (m^2/s)
k_{in}	intrinsic permeability (m^2)
K^{ap}	apparent permeability (m/s)
K_{lq}^{rel}	relative permeability to liquid (–)
K_{gz}^{rel}	relative permeability to gas (–)
K_{un}	undrained bulk modulus (Pa)
K_0	drained bulk modulus (Pa)
K_{lq}	inverse of compressibility of liquid water (Pa)
K_s	inverse of compressibility of solid (Pa)
M	Biot modulus (Pa)
M_{vp}^{ol}	molar mass of vapour (kg/mol)
M_{da}^{ol}	molar mass of dry air (kg/mol)
M_{lq}	total mass of liquid contained the sample (drying test) (kg)
M_{lq}^{u}	total mass of liquid contained in upstream reservoir (kg)
M_{lq}^{d}	total mass of liquid contained in downstream reservoir (kg)
$\boldsymbol{M}_{lq}$	specific liquid velocity vector (kg/m^2/s)
$\boldsymbol{M}_{da}$	specific dry air velocity vector (kg/m^2/s)
$\boldsymbol{M}_{gz}$	specific gas velocity vector (kg/m^2/s)
$\boldsymbol{M}_{vp}$	specific vapour velocity vector (kg/m^2/s)
m_{lq}	volumetric mass content of liquid (kg/m^3)
m_{da}	volumetric mass content of dry air (kg/m^3)
m_{vp}	volumetric mass content of vapour (kg/m^3)
M_{mes}	total number of measured data points (–)
N	poroelastic constant (Pa)
p_{atm}	atmospheric pressure (Pa)
p_{cp}	capillary pressure (Pa)
p_{lq}	liquid pressure (Pa)
p_{gz}	gas pressure (Pa)
p_{da}	dry air pressure (Pa)
p_{vp}	water vapour pressure (Pa)
p_{vp}^{sat}	saturated water vapour pressure (Pa)
R	universal perfect gas constant (J/kg/mol)
S_s	storage coefficient (1/Pa)
S_{re}^{u}	upstream reservoir storage coefficient (Pa m^2)
S_{re}^{d}	downstream reservoir storage coefficient (Pa m^2)
s	Laplace variable (1/s)
T	temperature (K)
t	dimensional time (s)
t^*	dimensionless time (–)
z	dimensional axial coordinate (–)
z^*	dimensionless axial coordinate (–)

Greek symbols

β	dimensionless parameter (pulse) (–)
ε_v	volumetric deformation (–)
γ	ratio of reservoir compressibilities (pulse) (–)
γ_{lq}	volumetric weight of liquid (N/m^3)
λ_{lq}	liquid conductivity (m^2/Pa/s)
λ_{gz}	gas conductivity (m^2/Pa/s)
μ_{lq}	dynamic liquid viscosity (Pa m)
μ_{gz}	dynamic gas viscosity (Pa m)
ω	dimensionless pore pressure in pulse test (–)
Ω	volume of the sample (m^3)
ϕ	porosity (–)
π	equivalent pore pressure (Pa)
ρ_{lq}	volumetric mass of liquid (kg/m^3)
ρ_{da}	volumetric mass of dry air (kg/m^3)
ρ_{vp}	volumetric mass of vapour (kg/m^3)
θ	theoretical value
θ_{mes}	experimental data
σ_m	mean stress (Pa)
ζ^{u}	volume of liquid contained in upstream reservoir (m^3)
ζ^{d}	volume of liquid contained in downstream reservoir (m^3)
$\jmath$	cost functional (–)

Subscripts

0	initial state
∞	asymptotic value state (drying test)

Superscript

imp	imposed value (drying test)

that the permeability of many clayey formations is apparently scale independent (or relative to the intrinsic permeability). Consequently the understanding of the fluid transport rates in these low permeability rocks is of fundamental importance to study the waste isolation.

Because of the long period required for a single test for very low intrinsic permeability, the conventional measuring techniques such as constant-head are impracticable. Brace et al. [2] introduced a transient flow method to measure intrinsic permeability in the case of negligible specific storage of rocks. The specific storage coefficient of a rock sample, S_s, is defined as the volume of water, per unit volume of saturated rock, injected into the porosity when it is exposed to a unit increase of pore

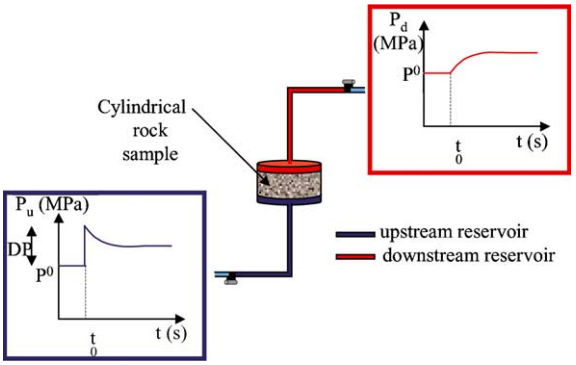

Fig. 1. Transient pulse technique.

fluid pressure. The specific storage is equally an important property for characterizing transient flow fluid [33,35,36]. Although the assumption of [2] may be reasonable for some crystalline rocks, Hsieh et al. [12] indicated that it is generally poor for rocks such as shales and argillite, which have significant porosity and compressive storage. These authors introduced the determination of the specific storage of the rock through the transient pulse test, and they presented a general analytical solution of the pulse test. A thin cylindrical rock sample connected to two fluid reservoirs (Fig. 1): the upstream reservoir and the downstream reservoir, is needed to conduct a pulse test. After the sample saturation and the pore pressure homogenization the pressure is suddenly increased in the upstream reservoir. Generally speaking the intrinsic permeability and the specific storage of the rock sample are deduced from comparison between the pressure evolution into the two reservoirs and theoretical curves.

1.2. Partially saturated case

The principle of the determination of the permeability in the partially saturated domain is based upon measures of weight loss and deformation of a sample during a drying test. The kinetic of variations of weight and deformation is linked to the permeability. Due to the presence of gas and also to hydromechanical couplings in rocks such as argillites, the coupled diffusion process in partially saturated domain is highly non-linear. Those equations are, in the general case of partially saturated porous media, highly non-linear due to the presence of gas and numerical methods such as finite element or finite volume have to be used to solve the direct problem [5,9]. Example of estimate of transfer parameter in concrete based on finite volume modelling of drying tests can be found in [16]. Pintado et al. [21] present results for coupled thermal–hydric parameters of a bentonite based upon finite element modelling for direct problem and inverse problem theory for identification. In this paper a linearization method applied to drying tests developed by Olchitzky [18] for a swelling clay has been adapted for the argillites and used to obtain order of magnitude of the permeability in the partially saturated domain.

2. Coupled hydromechanical model

2.1. Constitutive equations for the partially saturated medium

Let a porous medium be composed of a deformable matrix, and be partially saturated by an incompressible liquid (subscript lq) in equilibrium with its vapour (subscript vp), while the vapour forms an ideal mixture (subscript gz) with another gas (dry air, subscript da). A phase change between the liquid and its vapour is possible. Darcy's laws and Fick's laws are respectively taken into account to model the diffusion of the mixture (dry air and vapour), the liquid, and the diffusion of the vapour in the mixture. Assuming isothermal conditions, the linear porous elastic model consists of three balance equations: dry air mass, water species mass (both liquid and vapour) and linear momentum of the multiphase media. The non-linear isotropic poroelastic constitutive equations for partially saturated media (see Ref. [6]) can be written incrementally as ($\alpha, \beta = \mathrm{lq}, \mathrm{vp}, \mathrm{da}$, summation on β):

$$\mathrm{d}\sigma_{\mathrm{m}} = K_0\,\mathrm{d}\varepsilon_{\mathrm{v}} - b_\alpha\,\mathrm{d}p_\alpha$$
$$\mathrm{d}\sigma_{\mathrm{m}} = K_{\mathrm{un}}\,\mathrm{d}\varepsilon_{\mathrm{v}} - b_\alpha M_{\alpha\beta}\frac{\mathrm{d}m_\beta}{\rho_\beta} \tag{1}$$

$$\mathrm{d}s_{ij} = 2G\,\mathrm{d}e_{ij} \tag{2}$$

$$\mathrm{d}p_\alpha = M_{\alpha\beta}\left(-b_\beta\,\mathrm{d}\varepsilon_{\mathrm{v}} + \frac{\mathrm{d}m_\beta}{\rho_\beta}\right) \tag{3}$$

where σ_{m}, $\mathbf{s}$, ε_{v}, $\mathbf{e}$, m_i, ρ_i, p_i denote respectively the mean stress, the deviatoric stress tensor, volumetric strain, the deviatoric strain tensor, the fluid mass supplies, the partial pressures and the density of the constituents (l, v, a). K_0 and K_{un} denote respectively the drained ($\mathrm{d}p_i = 0$ for $i = \mathrm{lq}$, vp, da) and *undrained* bulk moduli ($\mathrm{d}m_i = 0$, for $i = \mathrm{lq}$, vp, da), b_i and M_{ij} represent Biot coefficients and Biot moduli for unsaturated poroelastic media. By inverting Eqs. (3), fluid mass supplies can be expressed in terms of partial pressures and volumetric strain:

$$\frac{\mathrm{d}m_\alpha}{\rho_\alpha} = b_\alpha\,\mathrm{d}\varepsilon_{\mathrm{v}} + N_{\alpha\beta}\,\mathrm{d}p_\beta \tag{4}$$

The deviatoric behaviour equation (2) is not coupled to the volume change behaviour equation (1). In the general case, bulk moduli, Biot coefficients b_α, Biot moduli $M_{\alpha\beta}$ and $N_{\alpha\beta}$ coefficients are functions of volumetric

strain, partial pressures p_α and temperature. Experimental determination of poroelastic parameters b_α, $N_{\alpha\beta}$, $M_{\alpha\beta}$ for materials such as concrete and clays is discussed in Ref. [19]. Detailed expressions of b_i and $N_{\alpha\beta}$ coefficients are given in Appendix A. Biot coefficients b_α and $N_{\alpha\beta}$ are functions of partial pressures p_α, liquid saturation S_{lq}, the derivative of liquid saturation relative to capillary pressure $p_{\mathrm{cp}} = p_{\mathrm{gz}} - p_{\mathrm{lq}}$ and a constant coefficient b (Biot's constant). Dry air pressure p_{da} can be expressed in terms of total gas pressure and vapour pressure $p_{\mathrm{da}} = p_{\mathrm{gz}} - p_{\mathrm{vp}}$. The vapour pressure can be eliminated using the thermodynamic equilibrium relation between water liquid and water vapour [6]:

$$\frac{p_{\mathrm{vp}}}{p^0_{\mathrm{vp}}} = \exp\left(\frac{M^{\mathrm{ol}}_{\mathrm{vp}}}{\rho_{\mathrm{lq}} RT}(p_{\mathrm{lq}} - p^0_{\mathrm{lq}})\right) \tag{5}$$

where the index 0 refers to a saturated reference state ($p^0_{\mathrm{cp}} = 0$, $p^0_{\mathrm{lq}} = p^0_{\mathrm{gz}} = p_{\mathrm{atm}}$), $M^{\mathrm{ol}}_{\mathrm{vp}}$, R and h_{r} respectively represent the molar vapour mass the universal gas constant and the relative humidity. p^0_{vp} denotes the vapour pressure in a water saturated air ($p_{\mathrm{lq}} = p_{\mathrm{gz}} = p_{\mathrm{atm}}$). It is a function of the temperature (T in Kelvin) which can be calculated thanks to the relation (Ref. [3]):

$$p^0_{\mathrm{vp}} = p^{\mathrm{sat}}_{\mathrm{vp}}(T) = 10^{2.7858 + \frac{T-273.5}{31.559+0.1354(T-273.5)}} \tag{6}$$

Two independent pressures can be chosen as state variables between liquid pressure, gas pressure, and capillary pressure.

2.2. Conduction equations for multiphase flow

By applying Darcy's generalised law for multiphase flow in unsaturated media, the velocity of liquid and the average relative molar velocity of gas mixture are governed by (gravity is neglected):

$$\frac{\boldsymbol{M}_{\mathrm{lq}}}{\rho_{\mathrm{lq}}} = -\lambda_{\mathrm{lq}} \nabla \boldsymbol{p}_{\mathrm{lq}} \tag{7}$$

$$\frac{\boldsymbol{M}_{\mathrm{gz}}}{\rho_{\mathrm{gz}}} = -\lambda_{\mathrm{gz}} \nabla \boldsymbol{p}_{\mathrm{gz}} \tag{8}$$

where λ_{lq} and λ_{gz} denote respectively Darcy's conductivity for liquid and gas:

$$\lambda_{\mathrm{lq}} = \frac{k_{\mathrm{in}} K^{\mathrm{rel}}_{\mathrm{lq}}(S_{\mathrm{lq}})}{\mu_{\mathrm{lq}}}, \quad \lambda_{\mathrm{gz}} = \frac{k_{\mathrm{in}} K^{\mathrm{rel}}_{\mathrm{gz}}(S_{\mathrm{lq}})}{\mu_{\mathrm{gz}}} \tag{9}$$

k_{in}, $K^{\mathrm{rel}}_{\mathrm{lq}}$, $K^{\mathrm{rel}}_{\mathrm{gz}}$, μ_{lq}, μ_{gz}, F denote respectively the intrinsic and relative permeabilities to liquid and gas, and dynamic viscosities. The diffusion of the vapour in the gas mixture is taken into account using Fick's law:

$$\frac{\boldsymbol{M}_{\mathrm{vp}}}{\rho_{\mathrm{vp}}} - \frac{\boldsymbol{M}_{\mathrm{da}}}{\rho_{\mathrm{da}}} = -F \nabla \boldsymbol{C}_{\mathrm{vp}}, \quad C_{\mathrm{vp}} = \frac{p_{\mathrm{vp}}}{p_{\mathrm{gz}}} \tag{10}$$

where F represents Fick's coefficient (see Refs. [16,20, 29]). By combining the Darcy and Fick relations two conduction laws can be written for water liquid, water vapour and dry air in terms of capillary and gas pressure gradients:

$$\boldsymbol{M}_{\mathrm{lq}} + \boldsymbol{M}_{\mathrm{vp}} = -K_{\mathrm{lc}} \nabla \boldsymbol{p}_{\mathrm{cp}} - K_{\mathrm{lg}} \nabla \boldsymbol{p}_{\mathrm{gz}} \tag{11}$$

$$\boldsymbol{M}_{\mathrm{da}} = -K_{\mathrm{gc}} \nabla \boldsymbol{p}_{\mathrm{cp}} - K_{\mathrm{gg}} \nabla \boldsymbol{p}_{\mathrm{gz}} \tag{12}$$

Detailed expression of coefficients K_i are given in Appendix A.

2.3. Momentum and diffusion equations

The linear momentum equation can be expressed as follows (by neglecting gravity):

$$\nabla \cdot \boldsymbol{\sigma} = \boldsymbol{0} \tag{13}$$

The mass conservation equations for the water species and dry air reads:

$$\begin{aligned} &\frac{\partial}{\partial t}[m_{\mathrm{lq}} + m_{\mathrm{vp}}] = -\nabla \cdot [\boldsymbol{M}_{\mathrm{lq}} + \boldsymbol{M}_{\mathrm{vp}}] \\ &\frac{\partial m_{\mathrm{da}}}{\partial t} = -\nabla \cdot [\boldsymbol{M}_{\mathrm{da}}] \end{aligned} \tag{14}$$

The field equations can be obtained by inserting Darcy's and Fick's conduction laws and also the constitutive poroelastic equations into Eqs. (13) and (14). The two non-linear diffusion equations take the form:

$$\begin{aligned} &C_{\mathrm{l}\varepsilon}\frac{\partial \varepsilon_{\mathrm{v}}}{\partial t} + C_{\mathrm{lc}}\frac{\partial p_{\mathrm{cp}}}{\partial t} + C_{\mathrm{lg}}\frac{\partial p_{\mathrm{gz}}}{\partial t} \\ &\quad = \nabla \cdot [K_{\mathrm{lc}} \nabla p_{\mathrm{cp}}] + \nabla \cdot [K_{\mathrm{lg}} \nabla p_{\mathrm{gz}}] \end{aligned} \tag{15}$$

$$\begin{aligned} &C_{\mathrm{g}\varepsilon}\frac{\partial \varepsilon_{\mathrm{v}}}{\partial t} + C_{\mathrm{gc}}\frac{\partial p_{\mathrm{cp}}}{\partial t} + C_{\mathrm{gg}}\frac{\partial p_{\mathrm{gz}}}{\partial t} \\ &\quad = \nabla \cdot [K_{\mathrm{gc}} \nabla p_{\mathrm{cp}}] + \nabla \cdot [K_{\mathrm{gg}} \nabla p_{\mathrm{gz}}] \end{aligned} \tag{16}$$

where C_{ij} and K_{ij} coefficients are functions of prime variables (see Appendix A for detailed expressions). In what follows, gravity terms will be neglected.

2.4. Constitutive equations for the fully saturated medium

The limiting saturated case is obtained by introducing the following conditions:

$$\begin{aligned} &p_{\mathrm{cp}} \to 0 \\ &S_{\mathrm{lq}}(p_{\mathrm{cp}}) \to S_{\mathrm{lq}}(0) = 1 \\ &\frac{\partial S_{\mathrm{lq}}(p_{\mathrm{cp}})}{\partial p_{\mathrm{cp}}} \to \left[\frac{\partial S_{\mathrm{lq}}}{\partial p_{\mathrm{cp}}}\right]_{p_{\mathrm{cp}}=0} = 0 \end{aligned} \tag{17}$$

in the general constitutive equations (1), (4) and (3). Finally, the diffusion equation can be simply expressed as:

$$b\frac{\partial \varepsilon_v}{\partial t}+\left(N+\frac{\phi}{K_{lq}}\right)\frac{\partial p_{lq}}{\partial t}=\lambda_{lq}\nabla\cdot[\nabla p_{lq}] \tag{18}$$

or in terms of mean stress σ_m:

$$\frac{b}{K_0}\frac{\partial \sigma_m}{\partial t}+\left(N+\frac{\phi}{K_{lq}}+\frac{b^2}{K_0}\right)\frac{\partial p_{lq}}{\partial t}=\lambda_{lq}\nabla\cdot[\nabla p_{lq}] \tag{19}$$

where

$$N+\frac{\phi}{K_{lq}}+\frac{b^2}{K_0}=\frac{K_{un}}{MK_0} \tag{20}$$

$$\frac{1}{M}=N+\frac{\phi}{K_{lq}} \tag{21}$$

M is the Biot modulus of the saturated porous medium and K_{un} is the undrained bulk modulus.

2.5. Relation between poroelastic and classical transfer parameters

The uncoupling hydraulic diffusion equation is classically written in terms of specific storage coefficient S_s and apparent permeability K^{ap}:

$$S_s\frac{\partial p_{lq}}{\partial t}-K^{ap}\nabla\cdot[\nabla p_{lq}]=0 \tag{22}$$

The relation between hydraulic conductivity λ_{lq} and apparent permeability K^{ap} in the saturated case:

$$\lambda_{lq}=\frac{k}{\mu_{lq}}=\frac{K^{ap}}{\gamma_{lq}} \tag{23}$$

and the comparison between the uncoupling equation (22) and the hydromechanical coupling equations (18) and (19) allows to express the specific storage coefficient S_s in terms of poroelastic coefficients in two particular cases. For a test with zero deformation (18) one obtains:

$$S_s^{\varepsilon}=\gamma_{lq}\frac{1}{M} \tag{24}$$

and for a test with constant mean stress:

$$S_s^{\sigma}=\gamma_{lq}\frac{1}{M}\frac{K_{un}}{K_0} \tag{25}$$

The ratio between the two specific storage coefficient is given by the ratio between undrained and drained bulk moduli:

$$\frac{S_s^{\sigma}}{S_s^{\varepsilon}}=\frac{K_{un}}{K_0} \tag{26}$$

As an example, in the case of the argillite studied in this paper, the poroelastic data $b=0.75$, $\phi=0.1$, $K_0=4000$ MPa, $K_{lq}=2200$ MPa, $M=11\,600$ MPa, $K_{un}=K_0+b^2M=10\,525$ MPa one obtains:

$$S_s^{\sigma}\approx 2.6S_s^{\varepsilon} \tag{27}$$

This numerical application shows the possible importance of hydromechanical couplings and it gives also order of magnitude of specific storage coefficient. It will be noticed in the next section that the correct condition for the pulse test is more close to constant stress than to zero deformation. The corresponding expression (25) will be used in the rest of the paper.

3. Pulse test for the saturated case

3.1. Initial and boundary conditions

One considers a cylindrical sample of radius R and height L submitted to hydrostatic stress. Initially, the sample is saturated and the liquid pressure and mean stress inside the sample are homogeneous (p_{lq}^0, σ_m^0):

$$p_{lq}(\boldsymbol{x},t=0)=p_{lq}^0 \tag{28}$$

$$\sigma_m(\boldsymbol{x},t=0)=\sigma_m^0 \tag{29}$$

where $\boldsymbol{x}$ represents the position vector. The lateral surface Γ_R of the sample is insulated:

$$\boldsymbol{M}_{lq}\cdot\boldsymbol{n}=0 \quad \text{on } \Gamma_R \tag{30}$$

The liquid pressure is suppose homogeneous in the two reservoirs: downstream reservoir ($z=0$) and upstream reservoir ($z=L$) where z denotes the axial coordinate:

$$\begin{aligned} &p_{lq}(\boldsymbol{x},t)=p_{re}^{u}(t) \quad \text{on } \Gamma_L\\ &p_{lq}(\boldsymbol{x},t)=p_{re}^{d}(t) \quad \text{on } \Gamma_0 \end{aligned} \tag{31}$$

A sudden increment of liquid pressure, is carried out in the upstream reservoir:

$$p_{re}^{u}(0^+)=p_{lq}^0+\Delta p \tag{32}$$

The conservation of liquid mass give the two boundary conditions between the sample and the reservoirs:

$$\begin{aligned} &\frac{\partial \zeta^u}{\partial t}=\int_{\Gamma_L}-\lambda_{lq}\nabla p_{lq}(\boldsymbol{x},t)\cdot\boldsymbol{n}\,da\\ &\frac{\partial \zeta^d}{\partial t}=\int_{\Gamma_0}-\lambda_{lq}\nabla p_{lq}(\boldsymbol{x},t)\cdot\boldsymbol{n}\,da\\ &\zeta^u=\frac{M_{lq}^u}{\rho_{lq}},\quad \zeta^d=\frac{M_{lq}^d}{\rho_{lq}} \end{aligned} \tag{33}$$

M_{lq}^u, M_{lq}^d, ζ^u and ζ^d denote respectively the mass and volume of liquid contained in the upstream and downstream reservoirs. By assuming a linear relation between the volume of liquid content in the reservoir and the liquid pressure:

$$\zeta^u=\frac{p_{re}^u}{C_{re}^u},\quad \zeta^d=\frac{p_{re}^d}{C_{re}^d} \tag{34}$$

The two coefficients C_{re}^u and C_{re}^d represent the compressibilities of the reservoirs and can be expressed to

the usual reservoir storage coefficients S_{re}^{u} and S_{re}^{d} by relations (see Ref. [12]):

$$C_{re}^{u}=\frac{S_{re}^{u}}{\gamma_{lq}},\quad C_{re}^{d}=\frac{S_{re}^{d}}{\gamma_{lq}} \tag{35}$$

The boundary condition between reservoirs and sample can be written as:

$$\begin{aligned}
&\int_{\Gamma_L}-\lambda_{lq}\nabla p_{lq}(\boldsymbol{x},t)\cdot\boldsymbol{n}\,da=\frac{1}{C_{re}^{u}}\frac{\partial p_{lq}(\boldsymbol{x},t)}{\partial t}\\
&p_{lq}(\boldsymbol{x},t)=p_{re}^{u}(t)\quad\text{on }\Gamma_L\\
&\int_{\Gamma_0}-\lambda_{lq}\nabla p_{lq}(\boldsymbol{x},t)\cdot\boldsymbol{n}\,da=\frac{1}{C_{re}^{d}}\frac{\partial p_{lq}(\boldsymbol{x},t)}{\partial t}\\
&p_{lq}(\boldsymbol{x},t)=p_{re}^{d}(t)\quad\text{on }\Gamma_0
\end{aligned} \tag{36}$$

3.2. A simplified approach: hypothesis of constant mean stress

Due to the coupling between hydraulic and mechanical behaviour this problem is generally three-dimensional, or two-dimensional with axial symmetry. The rigorous method to solve this problem is to perform coupled hydromechanical calculations by using finite element code for example. Finite element modelling have been performed on this problem and comparisons between 2D-axisymmetrical and 1D analysis show that hypothesis of constant mean stress in the sample and one-dimensional flow is correct (relative error on pore pressure in lower than 15%). The only space variable of this problem is the vertical coordinate z and the equation to solve can be written as:

$$\frac{K_{un}}{MK_0\lambda_{lq}}\frac{\partial p_{lq}}{\partial t}-\frac{\partial^2 p_{lq}}{\partial z^2}=0 \tag{37}$$

$$\left[\frac{\partial p_{lq}}{\partial z}\right]_{z=0}=\frac{1}{\pi R^2 C_{re}^{d}\lambda_{lq}}\frac{dp_{re}^{d}(t)}{dt} \tag{38}$$

$$\left[\frac{\partial p_{lq}}{\partial z}\right]_{z=L}=-\frac{1}{\pi R^2 C_{re}^{u}\lambda_{lq}}\frac{dp_{re}^{u}(t)}{dt} \tag{39}$$

By introducing dimensionless variables:

$$z^*=\frac{z}{L},\quad t^*=\frac{Dt}{L^2},\quad \omega=\frac{p_{lq}-p_{lq}^{0}}{\Delta p} \tag{40}$$

$$D=\frac{\lambda_{lq}MK_0}{K_{un}} \tag{41}$$

$$\beta=\frac{\pi R^2 L C_{re}^{u}K_{un}}{MK_0},\quad \gamma=\frac{C_{re}^{u}}{C_{re}^{d}} \tag{42}$$

the problem to solve can be written:

$$\begin{aligned}
&\frac{\partial\omega}{\partial t^*}-\frac{\partial^2\omega}{\partial z^{*2}}=0\\
&\left[\frac{\partial\omega}{\partial z^*}\right]_{z^*=0}-\frac{\gamma}{\beta}\frac{d\omega_{re}^{d}(t^*)}{dt^*}=0\\
&\left[\frac{\partial\omega}{\partial z^*}\right]_{z^*=1}+\frac{1}{\beta}\frac{d\omega_{re}^{u}(t^*)}{dt^*}=0\\
&\omega(z^*,0)=0\\
&\omega(1,t^*=0^+)=\omega_{re}^{u}(0^+)=1
\end{aligned} \tag{43}$$

Hsieh et al. [12] solved this initial-boundary value problem by the Laplace transform method. The solution of the system (43) in the Laplace transform space can be written as:

$$\bar{\omega}(z^*,s)=\frac{\beta\cosh(\sqrt{s}z^*)+\sqrt{s}\gamma\sinh(\sqrt{s}z^*)}{s\beta(1+\gamma)\cosh(\sqrt{s})+\sqrt{s}(\beta^2+s\gamma)\sinh(\sqrt{s})} \tag{44}$$

Three parameters D, β and γ control evolution of pressure in the two reservoirs. The solution in Laplace transform space (44) allows the three parameters D, β and γ to be identified. In this case the compressibilities of the up and down reservoirs (C_{re}^{u} and C_{re}^{d}) are known so identification of β determines the ratio MK_0/K_{un}. Finally the comparison between diffusivity D and the ratio MK_0/K_{un} gives the liquid conductivity λ_{lq}.

3.3. Parameter-identification technique: inverse problem solution

Neuzil et al. [17] offered a graphical method to carry out both hydraulic parameters (see Ref. [8] for details). A more rigorous and objective approach is given by the theory of inverse problem. The problem of parameter identification is an inverse problem, also known as back analysis (see Refs. [13,14,27]). Parameters-identification theory have been applied to various field or laboratory investigations [21,23,24,26]. The objective of the inverse problem is to quantified and minimizing the difference between experimental data and the corresponding computed value in order to obtain unknown parameters. In our case this method is applied to the identification of argillite hydraulic and poroelastic parameters using the difference between upstream and downstream pressure measurements as input data. Then, the objective function which quantify the difference between the experimental data and the corresponding theoretical value is given by Eq. (45). The following presentation is based upon Lecampion [13].

$$\begin{aligned}
&\jmath(\boldsymbol{c})=\frac{1}{2}\sum_{i=1}^{M_{mes}}w_i\left(\theta(\boldsymbol{c},t_i)-\theta_{mes}(t_i)\right)^2\\
&\theta(\boldsymbol{c},t_i)=\frac{p_{re}^{u}(\boldsymbol{c},t_i)-p_{re}^{d}(\boldsymbol{c},t_i)}{\Delta p}\\
&\theta_{mes}(t_i)=\frac{p_{mes}^{u}(t_i)-p_{mes}^{d}(t_i)}{\Delta p_{mes}}
\end{aligned} \tag{45}$$

where p^{u}_{mes}, p^{d}_{mes}, p^{u}_{re}, p^{d}_{re} denote respectively measured upstream and downstream pressure and calculated upstream and downstream pressure. M_{mes} is the total number of measured data points. w_i is a weight coefficient. The vector $\boldsymbol{c}$ contains the constitutive parameters to identify:

$$\boldsymbol{c} = \{K_{un}, K_0, M, \lambda_{lq}\} \tag{46}$$

On the basis of the previous section, this vector has been chosen equal to:

$$\boldsymbol{c} = \{D, \beta\} \tag{47}$$

The objective function can be written as:

$$\begin{aligned} &\jmath(\boldsymbol{c}) = \frac{1}{2}\boldsymbol{y}^{T}\cdot\boldsymbol{W}\cdot\boldsymbol{y} = \frac{1}{2}y_i W_{ij} y_j \\ &W_{ij} = W_{ji} \\ &y_i = \theta_i - \theta_i^{mes} \end{aligned} \tag{48}$$

By introducing a gradient matrix $\boldsymbol{A}$ and the Hessian matrix $\boldsymbol{Q}$ respectively composed by first and second derivative to parameters:

$$A_{ij} = \frac{\partial y_i}{\partial c_j}, \quad Q_{mn}(i) = \frac{\partial^2 y_i}{\partial c_m \partial c_n} \tag{49}$$

The second order expansion of the objective function $\jmath(\boldsymbol{c})$ can be written as:

$$\begin{aligned} \jmath(\boldsymbol{c}+\Delta\boldsymbol{c}) = \jmath(\boldsymbol{c}) + \Delta\boldsymbol{c}^{T}\cdot\nabla_{\boldsymbol{c}}\jmath(\boldsymbol{c}) + \frac{1}{2}\Delta\boldsymbol{c}^{T}\cdot\nabla^2_{\boldsymbol{c}}\jmath(\boldsymbol{c})\cdot\Delta\boldsymbol{c} \\ + O(\Delta\boldsymbol{c}^3) \end{aligned} \tag{50}$$

where

$$\begin{aligned} &\nabla_{\boldsymbol{c}}\jmath(\boldsymbol{c}) = \boldsymbol{A}^{T}\cdot\boldsymbol{W}\cdot\boldsymbol{y} \\ &\frac{\partial\jmath}{\partial c_j} = A_{ji}W_{ik}y_k \\ &\nabla^2_{\boldsymbol{c}}\jmath(\boldsymbol{c}) = \boldsymbol{A}^{T}\cdot\boldsymbol{W}\cdot\boldsymbol{A} + \sum_{i=1,M_{mes}}\boldsymbol{Q}(i)\cdot(\boldsymbol{W}\cdot\boldsymbol{y})_i \\ &\frac{\partial^2\jmath}{\partial c_i\partial c_j} = \frac{\partial^2 y_k}{\partial c_i\partial c_j}W_{kl}y_l + \frac{\partial y_k}{\partial c_j}W_{kl}\frac{\partial y_l}{\partial c_i} \end{aligned} \tag{51}$$

The stationary condition (zero gradient) of the objective function writes:

$$\nabla_{\boldsymbol{c}}\jmath(\boldsymbol{c}) + \nabla^2_{\boldsymbol{c}}\jmath(\boldsymbol{c})\cdot\Delta\boldsymbol{c} = \boldsymbol{0} \tag{52}$$

The minimisation problem is highly non-linear. Consequently an iterative minimisation approach is required. Generally the optimization procedures that use the gradient of the objective function are efficient. We used the modified version of the Gauss–Newton method due to Levenberg–Marquardt [10]. By neglecting second order derivative $Q_{mn}(i)$ and replacing them by a diagonal parameter λ

$$\nabla^2_{\boldsymbol{c}}\jmath(\boldsymbol{c}) \approx \boldsymbol{A}^{T}\cdot\boldsymbol{W}\cdot\boldsymbol{A} + \lambda\boldsymbol{I} \tag{53}$$

the linear system corresponding to the stationary condition of the objective function becomes:

$$\Delta\boldsymbol{c} = -\left(\boldsymbol{A}^{T}\cdot\boldsymbol{W}\cdot\boldsymbol{A} + \lambda\boldsymbol{I}\right)^{-1}\cdot(\boldsymbol{A}^{T}\cdot\boldsymbol{W}\cdot\boldsymbol{y}) \tag{54}$$

In this paper the weight coefficients W_{ij} has been chosen equal to unity:

$$\boldsymbol{W} = \boldsymbol{I}, \quad W_{ij} = \delta_{ij} \tag{55}$$

Exact calculations of partial derivatives have been performed in the Laplace transform domain to express coefficients of sensitivity vector $\boldsymbol{A}$. The Stehfest's algorithm [25] has been used to invert the Laplace transform and return to the time domain. Due to the use of a numerical method to invert the Laplace transform, the approach is then semi-analytical. The limiting case of small dimensionless time a values ($t^* < 4\times10^{-3}$) is treated thanks to a series solution method described by Carslaw and Jaeger [4].

4. Experimental results

4.1. Specimen

The samples were cored at a depth about 470 and 500 m in Callovo-Oxfordien. It is the potential sedimentary formation for a radioactive waste repository in Meuse/Haute-Marne (in France). The clay mineral content is about 40% (interstratified illite/smectite, illite, chlorite). We use a water chemistry close to the hypothetical pore water in order to avoid the water chemistry effects of the pore fluid on the permeability. In addition the water must be degassed to prevent bubbles formation. The total calculated porosity is about 15% but it overestimates the connecting porosity involved in the transport phenomenon. The right cylindrical samples are realized with a diamond core drill and precision grinding. The sample diameter is about 3.8×10^{-2} m for 1.5×10^{-2} m in length. A lot of care were taken to avoid the loss of water content until the permeability test.

4.2. Test procedures

The design of the original experimental device developed for argillites has been presented in Escoffier et al. [8]. The upstream and downstream reservoirs storage must be determined before the pulse test experiment. In order to isolate the upstream reservoir from the downstream reservoir an encapsulated cylindrical aluminium specimen is stand between the two end caps. Then a hydrostatic pressure is applied to ensure the insulation of both reservoirs and the compressive storage of both reservoirs could be easily determined. For the test conducted on these argillite the upstream volume reservoir was 3.06 cm^3 and the downstream volume reservoir was 2.54 cm^3. Their compressibilities are carry

out in the range of 1–7 MPa. For these testing conditions, the compressive storage of the reservoirs is practically constant. The measured compressibility in the upstream reservoir was about $C_{re}^{u} \approx 5\text{–}6\times10^{-15}$ m^3 Pa^{-1}. In addition the ratio of the downstream reservoir storage to the upstream reservoir storage was about $C_{re}^{d}/C_{re}^{u} \approx 1.4$.

4.3. Results

Several months were necessary to conduct tests on this very low permeability rock (for instance more than three weeks were required to saturate a thin sample). After the sample saturation the hydraulic properties of the argillite were determined under hydrostatic loading. The experimental pore pressure responses have been analysed by inverse method. The pulse test method has been performed on five samples. The intrinsic permeability and the specific storage have been obtained under three different effective hydrostatic loading ranging from 2 to 19 MPa. The results obtained for the first three samples are given in Table 1 (see also [8] for corresponding curves). For these test conditions, the intrinsic permeability and the specific storage coefficient do not decrease with the increase of the hydrostatic loading. Based on the reservoirs storage design devices, the reservoirs storages are well adapted to the sample dimensions and the argillite hydraulic properties. Results obtained for another sample are presented in Table 2 and Fig. 2. The diffusivity sensitivity of the sample pressure response is more influenced by the apparatus design than the permeability sensitivity. An important dispersion can be noticed on liquid diffusivity for the tested samples. Two orders of magnitude are observed between minimal and maximal diffusivity values ($3\times10^{-9} \leqslant D \leqslant 200\times10^{-9}$ m^2/s). Under these effective hydrostatic conditions the intrinsic permeability k_{in} and

Table 2
Results of saturated pulse test (sample 4)

Specimen 4	
Temperature T (K)	293
Depth H (m)	475
Porosity ϕ_0	0.16
Initial effective stress (Pa)	6.3×10^{6}
Liquid conductivity λ_{lq} (m^2/Pa/s)	5.13×10^{-18}
Liquid diffusivity D (m^2/s)	3.22×10^{-09}
Apparent liquid permeability $K=\gamma_{lq}\lambda_{lq}$ (m/s)	5.13×10^{-14}

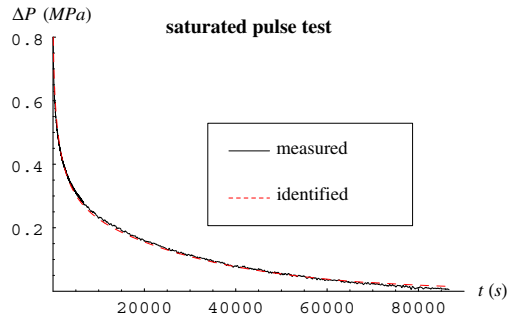

Fig. 2. Results of the pulse tests performed on the Meuse/Haute-Marne argillite.

Table 1
Results of saturated pulse tests (samples 1–2–3)

	Effective stress (10^6 Pa)					
	2.3	2.1	5	4.8	7.7	6.9
Specimen 1						
Liquid diffusivity D (10^{-09} m^2/s)	2.67	2.83	11.1	4.0	1.05	5.0
Liquid conductivity λ_{lq} (10^{-18} m^2/Pa/s)	8.0	8.5	10	8.0	4.2	5.0
Intrinsic permeability k_{in} (10^{-21} m^2)	8.0	8.5	10	8.0	4.2	5.0
	2.6	2.3	8.9	7.5	16.8	
Specimen 2						
Liquid diffusivity D (10^{-09} m^2/s)	20	23	28	37	37	
Liquid conductivity λ_{lq} (10^{-18} m^2/Pa/s)	18	23	25	30	15	
Intrinsic permeability k_{in} (10^{-21} m^2)	18	23	25	30	15	
	3	3	9	9	19	
Specimen 3						
Liquid diffusivity D (10^{-09} m^2/s)	200	200	133	40		
Liquid conductivity λ_{lq} (10^{-18} m^2/Pa/s)	40	30	20	20	40	
Intrinsic permeability k_{in} (10^{-21} m^2)	40	30	20	20	40	

the specific storage coefficient S_s respectively range from 0.4×10^{-20} to 12×10^{-20} m^2 and from 0.15×10^{-5} to 3×10^{-5} m^{-1}.

5. Drying tests for the partially saturated case

5.1. Experimental device design

The principle of the determination of the permeability of the argillite in the partially saturated domain is based upon measures of weight loss and deformation of a sample during a drying test. The kinetic of variations of weight and deformation is linked to the permeability. A cylindrical sample of radius R and height L of a partially saturated rock is introduce inside a hermetic chamber in which the relative humidity is maintained constant with a saline solution. The chosen dimensions of sample for experiments are $R \approx 25$ mm and $L \approx 20$ mm in order to obtain maximal exchange on bottom ($z = 0$) and top faces ($z = L$) relatively to lateral surface ($r = R$) and to minimize axial diffusion time. Due to the very little dimensions of the sample, the mass variations to measure are very small. As an example, a fully saturated sample with porosity $\phi = 0.15$ contains approximately $M_{lq} \approx 5.9$ g (mass of water liquid water) which gives the order of magnitude of the maximal mass variations during very long tests (several months). The main difficulty of theses tests on low permeable and low porosity rocks such as argillites is due to the very little mass variation to measure and then to the very high precision needed in weighing machine and in control of temperature and relative humidity in the hermetic chamber. A specific and original test device has been developed for these tests (see Fig. 3) (Table 3).

Table 3
Poroelastic data and dimensions

Depth (m)	500
Biot coefficient b	0.75
Drained bulk modulus K_0 (Pa)	4.0×10^9
Initial radius R_0 (m)	25×10^{-3}
Initial length L (m)	18×10^{-3}
Initial porosity ϕ_0	0.16

5.2. Initial and boundary conditions

Thanks to the Kelvin relation (see Eq. (5)), the relative humidity of the chamber corresponds to a capillary pressure imposed at the outer boundary of the sample. Initially, the sample is supposed to be in thermodynamical equilibrium with the air in the isolated chamber (of relative humidity h_r^0) so partially saturated and the capillary pressure, gas pressure, vapour pressure and mean stress inside the sample are homogeneous (p_i^0, σ_m^0). For a given saline solution, at a constant temperature $T = 293$ K, the initial pressures can be calculated thanks to the relations:

$$p_{cp}(\boldsymbol{x}, t=0) = -\frac{\rho_{lq} RT}{M_{vp}^{ol}} \ln(h_r^0) \tag{56}$$

$$p_{gz}(\boldsymbol{x}, t=0) = p_{atm} \tag{57}$$

$$p_{vp}(\boldsymbol{x}, t=0) = p_{vp}^{sat}(T) h_r^0 \tag{58}$$

$$\sigma_{ij}(\boldsymbol{x}, t=0) = -p_{atm}\delta_{ij} \tag{59}$$

At time $t = 0^+$, the saline solution is changed and the air in the chamber has a new relative humidity h_r^{imp}. This change induces a variation of the capillary pressure on the outer boundary of the sample (denoted $\partial\Omega$) which is supposed uniform:

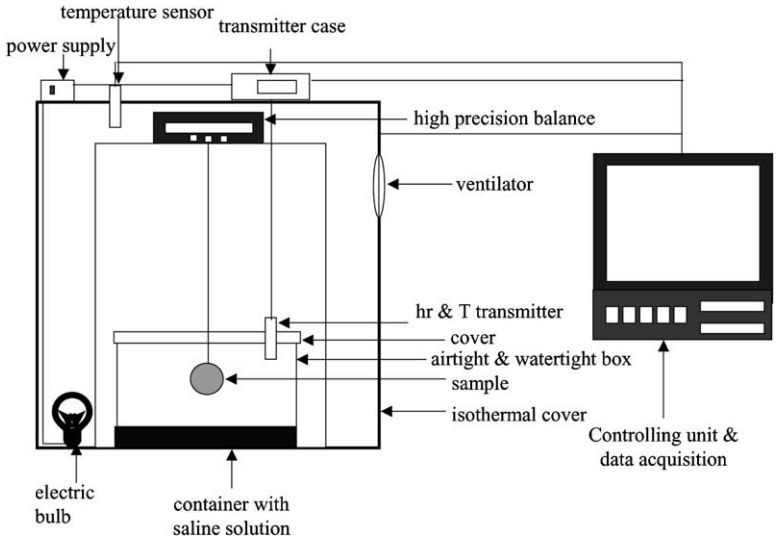

Fig. 3. Experimental device for permeability tests in partially saturated rocks.

$$\left[p_{\mathrm{cp}}(\boldsymbol{x}, t=0^{+})\right]_{\boldsymbol{x}\in\partial\Omega} = -\frac{\rho_{\mathrm{lq}} RT}{M_{\mathrm{vp}}^{\mathrm{ol}}} \ln(h_{\mathrm{r}}^{\mathrm{imp}}) \tag{60}$$

$$\left[p_{\mathrm{gz}}(\boldsymbol{x}, t=0^{+})\right]_{\boldsymbol{x}\in\partial\Omega} = p_{\mathrm{atm}} \tag{61}$$

$$\left[\sigma_n(\boldsymbol{x}, t=0^{+})\right]_{\boldsymbol{x}\in\partial\Omega} = -p_{\mathrm{atm}} \tag{62}$$

The direct problem is defined by Dirichlet hydraulic boundary conditions and by zero normal stress. It can be noticed that the real problem is simplified because the variation of capillary pressure on the outer boundary of the sample is supposed instantaneous. Due to coupling effects between Darcy and Fick diffusion processes, variations of gas pressure can be theoretically observed inside the sample. An increase of relative humidity induces swelling whereas a decrease of relative humidity induces shrinkage. The direct problem is defined by initial conditions, boundary conditions, and field equations constituted by momentum equation and diffusion equations for water and air (see Eqs. (13), (15), (16), (59) and (62)).

5.3. A simplified approach: one-dimensional linearized direct problem

As previously indicated the constitutive non-linear poroelastic model is strongly non-linear. Poroelastic coefficients, and diffusion coefficients are function depending on liquid saturation S_{lq} and its derivative, deformation, partial pressures and temperature. Furthermore, the highly non-linear character of the diffusion process for non-saturated porous materials such as argillite must not be under-evaluated so a direct linearization of transfer and equilibrium equations must be performed carefully. Another source of non-linearity is the non-reversible behaviour of the unsaturated porous materials: plasticity, damage, or plasticity coupled with damage are not taken into account in this paper (see [11]). Numerical methods such as finite element [15,28, 29], finite difference or finite volume methods [9,16,30] can be used to solve those non-linear partial differential equations. The linear poroelastic analysis presented in this section can be considered as a first approach. This approach does not aim to accurately characterize permeability but to obtain a correct order of magnitude on the basis of simplified assumptions. A linear model enables explicit solutions to be established and then make easier the solution of the inverse problem. The analytical method presented in this section has been obtained by Olchitzky [18] for the same problem of permeability determination in a Fo–Ca clay barrier. It will be noted that a similar analytical approach to the initially non-linear problem of heat-induced moisture movement in the vicinity of a spherical heat source has been presented by Basha and Selvadurai [1]. Another interesting analytical analysis of non-linear hygrothermal diffusion in unsaturated porous medium can be found in Yong et al. [34]. Analytical methods have to be used very carefully but they offer general insight into the physical phenomena and can be used to provide approximations of certain couplings effects. A recent linear approach to analysis of heat and moisture transfer in capillary porous media has been presented by Dantas et al. [7]. The linear poroelastic model is obtained by assuming that all functions N_{ij}, b_i, K_{ij}, ρ_i are constant, equal to the values of these functions calculated at the reference state denoted by index 0. Particularly in coupling coefficients, the liquid saturation S_{lq} and its derivative $\mathrm{d}S_{\mathrm{lq}}/\mathrm{d}p_{\mathrm{cq}}$ are taken as being constant, equal to $S_{\mathrm{lq}}^0 = S_{\mathrm{lq}}(p_{\mathrm{cp}}^0)$ and $S'_{\mathrm{lq}}0 = \mathrm{d}S_{\mathrm{lq}}/\ \mathrm{d}p_{\mathrm{cp}}(p_{\mathrm{cp}}^0)$. The liquid saturation is then a posteriori calculated by using the linearized saturation–capillary pressure curve:

$$S_{\mathrm{lq}}(p_{\mathrm{cp}}) = S_{\mathrm{lq}}^0 + S'_{\mathrm{lq}}0(p_{\mathrm{cp}} - p_{\mathrm{cp}}^0) \tag{63}$$

It must be emphasized that this approximation is valid only for small variations around the initial value p_{cp}^0. The hypothesises introduced by [18] to obtain an analytical solution for the problem of drying can be listed as follows: gas pressure is supposed to remain constant in the sample, equal to the atmospheric pressure p_{atm}, Fick diffusion is neglected $(F = 0)$ and then only Darcy relation for liquid (Eq. (7)) is used to describe the moisture transport, lateral face $(r = R)$ is supposed insulated so the flow of moisture is one-dimensional. Total mass variation is supposed equal to the liquid mass variation. The linearized poroelastic constitutive equation (4) becomes:

$$\frac{\mathrm{d}m_{\mathrm{lq}}}{\rho_{\mathrm{lq}}} = bS_{\mathrm{lq}}^0\,\mathrm{d}\varepsilon_{\mathrm{v}} - \left(\phi_0\left(\frac{S_{\mathrm{lq}}^0}{K_{\mathrm{lq}}} - S'_{\mathrm{lq}}0\right) + NS_{\mathrm{lq}}^{0^2}\right)\mathrm{d}p_{\mathrm{cp}} \tag{64}$$

The equations are similar to those of the consolidation problem for the saturated poroelastic medium (pore pressure equation, see Ref. [6]). By neglecting lateral liquid mass exchange and lateral deformation one obtains a one-dimensional coupled linear poroelastic problem to solve with initial and boundary conditions (taking into account symmetry):

$$\begin{aligned}
&p_{\mathrm{cp}}(z, t=0) = p_{\mathrm{cp}}^0\\
&\left[\frac{\partial p_{\mathrm{cp}}}{\partial z}\right](z=0, t>0) = 0\\
&\xi_z(z=0, t>0) = 0\\
&p_{\mathrm{cp}}(z=L/2, t>0) = p_{\mathrm{cp}}^{\mathrm{imp}} = p_{\mathrm{cp}}^{\infty}\\
&\sigma_{zz}(z=L/2, t>0) = -p_{\mathrm{atm}}
\end{aligned} \tag{65}$$

where ξ_z denotes the axial displacement. The momentum equation (13):

$$\frac{\partial \sigma_{zz}}{\partial z} = 0 \tag{66}$$

and linearized poroelastic constitutive equations (1) and (2) give:

$$\varepsilon_v = \frac{\partial \xi_z}{\partial z} = -\frac{bS_{lq}^0}{\lambda_0 + 2G}(p_{cp} - p_{cp}^0) \tag{67}$$

Relations (64) and (67) allows to express volumetric deformation in terms of capillary pressure. By integrating relation (64) one obtains:

$$\begin{aligned} &\frac{m_{lq} - m_{lq}^0}{\rho_{lq}} = -\eta_0(p_{cp} - p_{cp}^0) \\ &\eta_0 = \left(\frac{b^2}{\lambda_0 + 2G} + N\right)(S_{lq}^0)^2 + \phi_0\left(\frac{S_{lq}^0}{K_{lq}} - S_{lq}'^0\right) \end{aligned} \tag{68}$$

The parameter η_0 (unit Pa^{-1}) is similar to a specific heat coefficient for a thermal problem, or a specific storage coefficient in hydrogeology. It may be noticed that this is a coupled hydromechanical parameter so the identification of η_0 gives information on poromechanical coefficients (drained Lamé coefficients λ_0 and shear coefficient G). An increase of capillary pressure induces a weight loss and then a negative variation of liquid mass content. Finally the one-dimensional linear diffusion to solve can be written:

$$\begin{aligned} &\frac{\partial p_{cp}}{\partial t} - D_0\frac{\partial^2 p_{cp}}{\partial z^2} = 0 \\ &D_0 = \frac{\lambda_{lq}^0}{\eta_0} \end{aligned} \tag{69}$$

The solution of this one-dimensional linear problem can be expressed with a serie (see [6]):

$$\begin{aligned} &p_{cp}(z,t) - p_{cp}^0 = \left(p_{cp}^{imp} - p_{cp}^0\right)\left[1 - \sum_{n=0}^{\infty} Y_n(t)\right] \\ &Y_n(t) = \frac{4(-1)^{n+1}}{(2n+1)\pi}\cos(\omega_n z)\exp(-D_0\omega_n^2 t) \\ &\omega_n = \frac{(2n+1)\pi}{L} \end{aligned} \tag{70}$$

By integrating the volumetric liquid mass content over the initial volume of the sample one obtains the total liquid mass variation:

$$\Delta M_{lq}(t) = 2\pi R^2 \int_0^{L/2} \left(m_{lq}(z,t) - m_{lq}^0\right) dz \tag{71}$$

and then ($\Omega = \pi R^2 L$):

$$\begin{aligned} &\Delta M_{lq}(t) = -\rho_{lq}\Omega\left(p_{cp}^{imp} - p_{cp}^0\right)\eta_0\left[1 - \sum_{n=0}^{\infty} E_n(t)\right] \\ &E_n(t) = \frac{8}{(2n+1)^2\pi^2}\exp\left(-\frac{\lambda_{lq}^0}{\eta_0}\omega_n^2 t\right) \end{aligned} \tag{72}$$

5.4. Experimental results and identification

A sample cored at a depth about 500 m, as the specimen number 3 previously studied by pulse test in saturated conditions, in clayey Callovo-Oxfordien has been firstly submitted to an initial constant relative humidity $h_r^0 = 98\%$ in an hermetic chamber. The saline solution in the hermetic chamber $CuSO_4 \cdot 5H_2O$ has been replaced by KNO_3 in order to impose a decrease of relative humidity ($h_r^{imp} = 93\%$). Data relative to this test are recalled in Table 4: it is the test denoted A. After the test A, the same sample has been submitted a long time to a new relative humidity $h_r^{imp} = 85\%$ imposed by the saline solution KCl which corresponds to the initial condition of the test B. The saline solution in the hermetic chamber KCl has been replaced by NaCl to impose a new decrease of relative humidity ($h_r^{imp} = 75\%$). The desorption curve of this material has been characterized thanks to a microgravimeter test (*GAETAN* test, see [22]). Experimental results have been fitted by using Vachaud–Vauclin function (Eq. (73), Refs. [31,32] and Figs. 4 and 5):

$$S_{lq}(p_{cp}) = \frac{a_{vv}}{a_{vv} + \left(\frac{p_{cp}}{10^4}\right)^{b_{vv}}}, \quad a_{vv} = 13929.1, \quad b_{vv} = 1.038 \tag{73}$$

During the test, the total mass of the sample is regularly measured. Under the hypothesis of the study, variations of mass of gas and vapour are neglected and the total mass variation is supposed equal to the total liquid mass variation in the sample. The $\boldsymbol{c}$ vector of the constitutive parameters to identify has been chosen equal to:

$$\boldsymbol{c} = \{\lambda_{lq}^0, \eta_0\} \tag{74}$$

The first parameter, the liquid conductivity, mainly controls the transient evolution whereas the second parameter, η_0, is linked to the asymptotic (or maximal) liquid mass exchange. The relative variation of the total mass has been used for identification procedure:

$$\begin{aligned} &\theta(\boldsymbol{c}, t_i) = \frac{\Delta M_{lq}(t_i)}{M_0} \\ &\theta_{mes}(t_i) = \frac{M_{mes}(t_i) - M_0}{M_0} \end{aligned} \tag{75}$$

hence:

$$\begin{aligned} &\theta(\boldsymbol{c}, t_i) = -A_0\eta_0\left[1 - \sum_{n=1}^{\infty} E_n(t_i)\right] \\ &A_0 = \frac{\rho_{lq}\Omega_0\left(p_{cp}^{imp} - p_{cp}^0\right)}{M_0} \end{aligned} \tag{76}$$

The identification of the two parameters has been performed by using the optimization procedure described previously for the pulse test. In the case of the linearized

Table 4
Results of drying tests

	A	B
Temperature T (K)	293	293
Initial saline solution	$CuSO_4 \cdot 5H_2O$	KCl
Initial relative humidity h_r^0 (%)	98.0	85.1
Initial capillary pressure p_{cp}^0 (Pa)	2.77×10^6	9.51×10^6
Saline solution	KNO_3	NaCl
Imposed relative humidity h_r^{imp} (%)	93.2	75.4
Imposed capillary pressure p_{cp}^{imp} (Pa)	21.8×10^6	38.2×10^6
Initial saturation (calculated) S_{lq}^0	0.969	0.770
Asymptotic saturation (calculated) S_{lq}^∞	0.891	0.645
Volumetric deformation (calculated) ε_∞	-1.18×10^{-3}	-2.17×10^{-3}
Porosity variation (calculated) $\Delta\phi$	-9.25×10^{-4}	-1.71×10^{-3}
Liquid conductivity λ_{lq}^0 (m^2/Pa/s)	1.88×10^{-18}	1.57×10^{-19}
Equivalent specific storage coefficient η_0 (1/Pa)	1.50×10^{-9}	1.33×10^{-09}
Liquid diffusivity D (m^2/s)	1.25×10^{-9}	1.18×10^{-10}
Apparent liquid permeability $K=\gamma_{lq}\lambda_{lq}^0$ (m/s)	1.88×10^{-14}	1.57×10^{-15}

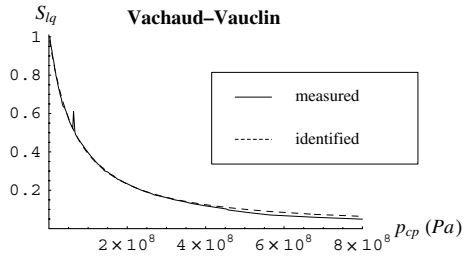

Fig. 4. Sorption curve for the argillite (micrograviméter test).

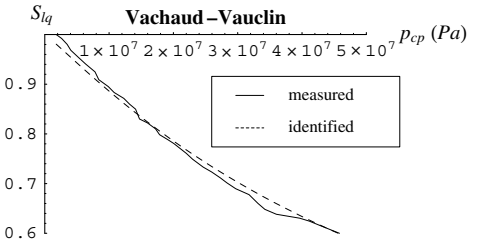

Fig. 5. Sorption curve for the argillite (micrograviméter test).

drying test, the sensitivity vector is calculated by deriving the analytical solution (76):

$$\frac{\partial\theta(\boldsymbol{c},t_i)}{\partial\lambda_{lq}^0}=A_0\eta_0\sum_{n=1}^{\infty}\frac{\partial E_n(t_i)}{\partial\lambda_{lq}^0} \tag{77}$$

$$\frac{\partial\theta(\boldsymbol{c},t_i)}{\partial\eta_0}=-A_0\left(1-\sum_{n=1}^{\infty}E_n(t_i)-\eta_0\sum_{n=1}^{\infty}\frac{\partial E_n(t_i)}{\partial\eta_0}\right) \tag{78}$$

$$\frac{\partial E_n(t_i)}{\partial\lambda_{lq}^0}=-\frac{8t_i}{L^2\eta_0}\exp\left(-\frac{\lambda_{lq}^0}{\eta_0}\omega_n^2t_i\right) \tag{79}$$

$$\frac{\partial E_n(t_i)}{\partial\eta_0}=\frac{8\lambda_{lq}^0t_i}{L^2\eta_0^2}\exp\left(-\frac{\lambda_{lq}^0}{\eta_0}\omega_n^2t_i\right) \tag{80}$$

On the basis of the linearization process, the initial value of η_0 parameter is calculated thanks to relation (68). Identification have been performed in two steps. A first step corresponding to optimization on one parameter, liquid conductivity λ_{lq}^0 by keeping η_0 constant, which gives the initial values $\lambda_{lq}^{0(0)}$ and $\eta_0^{(0)}$ for the second step: optimization process on the two parameters. Results of identification are summarized in Table 4. Measures and

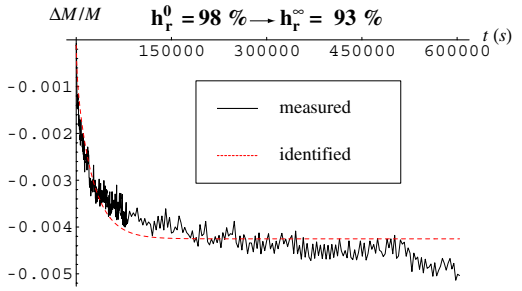

Fig. 6. Relative mass variation for imposed relative humidity 93%.

identified relative mass variations are compared in Figs. 6 and 7. It can be noticed that a decrease of liquid permeability of approximately one order of magnitude can be observed by comparing the two ranges of relative humidity. A third test will be performed, on the same sample, with lower relative humidities. It will be used to identify relative permeability to liquid. Comparisons between saturated and partially saturated tests show

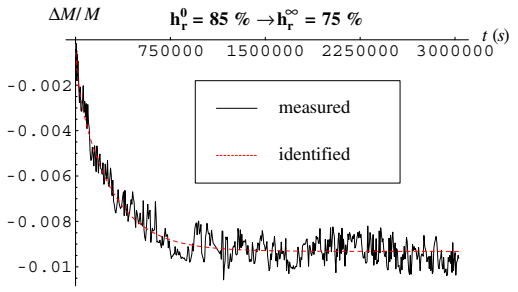

Fig. 7. Relative mass variation for imposed relative humidity 75%.

that liquid diffusivity and liquid permeability decrease with a decrease of liquid saturation. Other tests in saturated and partially conditions have to be performed to obtain more precise conclusions.

6. Conclusions

Experimental apparatus design is of fundamental importance to ensure the sensitivity of a pulse test experiment with respect to the intrinsic permeability and specific storage coefficient of a rock sample. First of all the experimental setup must take into account the ratio of the sample storage to the upstream reservoir storage. Secondly the time response which is linked to the intrinsic permeability must ranging from several hours to one day depending on the experimental device limits. Pressure sensitivity study, with respect to both hydraulic parameters, indicates that the specific storage sensitivity of the sample pressure response is more influenced by the apparatus design than the permeability sensitivity, but it does not take into account the response time. Anyway this approach indicates the part of the pressure response, which is the most influenced by both parameters. A back analysis of both parameters K^{ap} and S_s from pulse test is proposed. This inverse problem is based on an iterative minimisation approach of an objective function: the Levenberg–Marquardt method. The first derivatives of the error function with respect to hydraulics parameters are needed. There analytical expressions have been obtain through the Laplace transform domain. Then this method has been successfully applied on these very low permeability rocks.

Due to the very little dimensions of the tested samples, the low porosity and the very low permeability the mass variations to measure during drying tests are very small (lower than $1 \cdot g$ for the two cases presented!). It makes very difficult the design of the experimental device. Very high precision are needed in weighing device and in control of temperature and relative humidity in an hermetic chamber. The original test device developed has been used to obtain the first results presented in this paper. Work actually under way concern the simplified hypothesises, linear models as well as one-dimensional geometries, adopted in this paper. More accurate determination of the permeability will be obtained by taking into account non-linearities neglected in this paper and also two-dimensional effects thanks to coupled hygromechanical finite element modellings.

The influence of the hydromechanical coupling in saturated and partially saturated cases, is mainly concentrated on equivalent storage coefficient, analogous to heat capacities for thermal problems. The identification method based upon transient tests, pulse tests as well as drying tests, allows to identify the diffusivity and then the storage coefficient and permeability. An error upon analysis of hydromechanical coupling induces an error in interpretation of storage coefficients and consequently in deduced permeability. From a poromechanical point of view, those transient tests are very important because they give information not only on transfer parameters but also on poromechanical parameters. In such a kind of materials with low but not negligible porosity, and very low permeability, coupled poromechanical experiments are very difficult to perform. As an example, some parameters such as drained coefficients, Biot coefficients or Biot moduli in the partially saturated case, cannot be directly measured in this kind of material. Coherent estimates or coherent ranges of variation of these parameters can only, in many cases, be deduced from coupled hydromechanical back analyses such as those presented in this paper.

Concerning the rheological model adopted for the argillites, the preliminary results show that the uncoupling hypothesis between saturation (which is supposed to depend only on capillary pressure) and deformation seems to be irrelevant.

Acknowledgements

This work has been supported by ANDRA, Scientific Division, 1/7 rue Jean Monnet, Châtenay-Malabry F-92290. The author express sincere appreciation to the organization, especially to Drs. Nasser Hoteit and Kun Su.

Appendix A

A.1. Poroelastic coefficients

By taking into account the hypothesis of perfect mixture of perfect gases, b_i and N_{ij} coefficients can be written as (see [19]):

$$b_{lq} = bS_{lq}, \quad b_{vp} = b_{da} = b_{gz} = b(1 - S_{lq}), \quad b = 1 - \frac{K_0}{K_s} \tag{A.1}$$

$$
\begin{aligned}
&N_{\mathrm{da\,vp}} = N_{\mathrm{vp\,da}} = N_{\mathrm{gz}} = N\phi(1-S_{\mathrm{lq}}) - N_{\mathrm{lq}}\\
&N_{\mathrm{lq\,vp}} = N_{\mathrm{lq\,da}} = N_{\mathrm{vp\,lq}} = N_{\mathrm{da\,lq}} = N_{\mathrm{lq}}\\
&N_{\mathrm{lq\,lq}} = NS_{\mathrm{lq}} + \frac{\phi S_{\mathrm{lq}}}{K_{\mathrm{lq}}} - N_{\mathrm{lq}}\\
&N_{\mathrm{vp\,vp}} = N_{\mathrm{gz}} + \frac{\phi(1-S_{\mathrm{lq}})}{p_{\mathrm{vp}}}\\
&N_{\mathrm{da\,da}} = N_{\mathrm{gz}} + \frac{\phi(1-S_{\mathrm{lq}})}{p_{\mathrm{da}}}\\
&N_{\mathrm{lq}} = \phi\frac{\partial S_{\mathrm{lq}}}{\partial p_{\mathrm{cp}}} + NS_{\mathrm{lq}}(1-S_{\mathrm{lq}})\\
&N = \frac{(1-b)(b-\phi)}{K_0}
\end{aligned}
\tag{A.2}
$$

K_{lq} and K_{s} respectively denote the bulk moduli of the liquid and the solid particles (or grain material).

A.2. Coupled conductivities

$$
\begin{aligned}
&K_{\mathrm{lc}} = \lambda_{\mathrm{lq}}\rho_{\mathrm{lq}} + \frac{F(p_{\mathrm{gz}}-p_{\mathrm{vp}})\rho_{\mathrm{vp}}^2}{p_{\mathrm{gz}}^2\rho_{\mathrm{lq}}}\\
&K_{\mathrm{lg}} = -\lambda_{\mathrm{lq}}\rho_{\mathrm{lq}} - \lambda_{\mathrm{gz}}\rho_{\mathrm{vp}} - \frac{F(p_{\mathrm{gz}}-p_{\mathrm{vp}})\rho_{\mathrm{vp}}(p_{\mathrm{gz}}\rho_{\mathrm{vp}}-p_{\mathrm{vp}}\rho_{\mathrm{lq}})}{p_{\mathrm{gz}}^3\rho_{\mathrm{lq}}}\\
&K_{\mathrm{gc}} = -\frac{Fp_{\mathrm{vp}}\rho_{\mathrm{da}}\rho_{\mathrm{vp}}}{p_{\mathrm{gz}}^2\rho_{\mathrm{lq}}}\\
&K_{\mathrm{gg}} = \rho_{\mathrm{da}}\left(-\lambda_{\mathrm{gz}} + \frac{Fp_{\mathrm{vp}}\left(-p_{\mathrm{vp}}+\frac{p_{\mathrm{gz}}\rho_{\mathrm{vp}}}{\rho_{\mathrm{lq}}}\right)}{p_{\mathrm{gz}}^3}\right)\\
&\rho_{\mathrm{da}} = \frac{M_{\mathrm{da}}^{\mathrm{ol}}(p_{\mathrm{gz}}-p_{\mathrm{vp}})}{RT}, \quad \rho_{\mathrm{vp}} = \frac{M_{\mathrm{vp}}^{\mathrm{ol}}p_{\mathrm{vp}}}{RT}
\end{aligned}
\tag{A.3}
$$

where $M_{\mathrm{da}}^{\mathrm{ol}}$ and $M_{\mathrm{vp}}^{\mathrm{ol}}$ respectively represent the molar mass of dry air and water vapour.

A.3. Coupled capacities

$$
\begin{aligned}
&C_{\mathrm{l}\varepsilon} = b\big(S_{\mathrm{lq}}(\rho_{\mathrm{lq}}-\rho_{\mathrm{vp}}) + \rho_{\mathrm{vp}}\big)\\
&C_{\mathrm{g}\varepsilon} = b(1-S_{\mathrm{lq}})\rho_{\mathrm{da}}\\
&C_{\mathrm{lc}} = -\left(\frac{(\phi+NK_{\mathrm{lq}})S_{\mathrm{lq}}\rho_{\mathrm{lq}}}{K_{\mathrm{lq}}}\right) + N_{\mathrm{lq}}(\rho_{\mathrm{lq}}-\rho_{\mathrm{vp}})\\
&\qquad - \frac{\phi(1-S_{\mathrm{lq}})\rho_{\mathrm{vp}}^2}{p_{\mathrm{vp}}\rho_{\mathrm{lq}}}\\
&C_{\mathrm{lg}} = \frac{(\phi+NK_{\mathrm{lq}})S_{\mathrm{lq}}\rho_{\mathrm{lq}}}{K_{\mathrm{lq}}} + N(1-S_{\mathrm{lq}})\rho_{\mathrm{vp}}\\
&\qquad + \frac{\phi(1-S_{\mathrm{lq}})\rho_{\mathrm{vp}}^2}{p_{\mathrm{vp}}\rho_{\mathrm{lq}}}\\
&C_{\mathrm{gc}} = \rho_{\mathrm{da}}\left(-N_{\mathrm{lq}} + \frac{\phi(1-S_{\mathrm{lq}})\rho_{\mathrm{vp}}}{(p_{\mathrm{gz}}-p_{\mathrm{vp}})\rho_{\mathrm{lq}}}\right)\\
&C_{\mathrm{gg}} = (1-S_{\mathrm{lq}})\rho_{\mathrm{da}}\left(N + \frac{\phi(\rho_{\mathrm{lq}}-\rho_{\mathrm{vp}})}{(p_{\mathrm{gz}}-p_{\mathrm{vp}})\rho_{\mathrm{lq}}}\right)
\end{aligned}
\tag{A.4}
$$

References

[1] H.A. Basha, A.P.S. Selvadurai, Heat-induced moisture transport in the vicinity of a spherical heat source, Int. J. Numer. Anal. Methods Geomech. 22 (12) (1998) 969–981.

[2] W.F. Brace, J.B. Walsh, W.T. Frangos, Permeability of granite under high pressure, J. Geophys. Res. 73 (2) (1968) 2225–2236.

[3] R. Cadiergues, Propriétés de l'air humide et de l'eau: justification de nouveaux choix, PROMOCLIM E, Etud. Thermiques Aérauliques 9 (E-1) (1978) 21–33.

[4] H.S. Carslaw, J.C. Jaeger, Conduction of Heat in Solids, Oxford University Press, London, 1959, p. 510.

[5] C. Chavant, S. Granet, D. Le Boulch, Modeling of a nuclear waste disposal: Numerical and practical aspects, in: Thimus et al. (Eds.), Biot Conference on Poromechanics II, Balkema, 2002, pp. 145–150, ISBN 90 5809 394 8.

[6] O. Coussy, Mechanics of Porous Continua, John Wiley and Sons, Chichester, England, 1995.

[7] L.B. Dantas, H.R.B. Orlande, R.M. Cotta, An inverse problem of parameter estimation for heat and mass transfer in capillary porous media, Int. J. Heat Mass Transfer 46 (2003) 1587–1598.

[8] S. Escoffier, F. Homand, A. Giraud, N. Hoteit, K. Su, Under stress permeability determination of the Meuse/Haute-Marne argillite, International Journal for Engineering Geology, submitted for publication.

[9] R. Eymard, T. Gallouet, R. Herbin, Finite volume methods, in: P.G. Ciarlet, J.L. Lions (Eds.), Handbook of Numerical Analysis, 2000.

[10] P.E. Gill, W. Murray, M.H. Wright, Practical Optimization, 1982.

[11] A. Giraud, J.F. Shao, N. Ata, Induced damage modelling of unsaturated drying deformable materials, in: Pande et al. (Eds.), Numerical Models in Geomechanics, NUMOG VII, Balkema, 1999, pp. 263–268.

[12] P.A. Hsieh, J.V. Tracy, C.E. Neuzil, J.D. Bredehoeft, S.E. Silliman, A transient laboratory method for determining the hydraulic properties of 'tight' rocks. I. Theory, Int. J. Rock Mech. Min. Sci. Geomech. Abstr. 18 (1981) 245–252.

[13] B. Lecampion, Sur l'identification des paramètres des lois de comportement des roches argileuses, PhD Thesis (in French), Ecole Polytechnique, France, 2002.

[14] B. Lecampion, A. Constantinescu, D. NguyenMinh, Parameter indentification for lined tunels in a viscoplastic medium, Int. J. Numer. Anal. Methods Geomech. (2002) 1191–1211.

[15] R.L. Lewis, B.A. Schrefler, The Finite Element Method in the Static and Dynamic Deformation and Consolidation of Porous Media, second ed., Wiley, Chichester, 1998.

[16] M. Mainguy, Modèles de diffusion non linéaires en milieux poreux, Application à la dissolution et au séchage des matériaux cimentaires, PhD Thesis (in French), ENPC, Paris, France, 1999.

[17] C.E. Neuzil, C. Cooley, S.E. Silliman, J.D. Bredehoeft, P.A. Hsieh, A transient laboratory method for determining the hydraulic properties of 'tight' rocks. II. Application, Int. J. Rock Mech. Min. Sci. Geomech. Abstr. 18 (1981) 253–258.

[18] E. Olchitzky, Couplage hydromécanique et perméabilité d'une argile gonflante non saturée sous sollicitations hydriques et thermiques courbe de sorption et perméabilité à l'eau, PhD Thesis (in French), ENPC, Paris, France, 2002.
[19] E. Olchitzky, P. Dangla, T. Lassabatère, O. Didry, L. Malinsky, Towards the evaluation of thermo-hydro-mechanical parameters in unsaturated clay barriers, in: 5th International Workshop on Key Issues in Waste Isolation Research, UPC, Balkema, Barcelona, 1988.
[20] S. Olivella, A. Gens, J. Carrera, Water phase change and vapour flow in low permeability unsaturated soils with capillary effects, in: 5th International Workshop on Key Issues in Waste Isolation Research, UPC, Balkema, Barcelona, 1988.
[21] X. Pintado, A. Ledesma, A. Lloret, Backanalysis of thermohydraulic bentonite properties from laboratory tests, in: Proceedings of UPC98, Barcelona, Spain, 1998.
[22] J.E. Poirier, M. Francois, J.M. Cases, Study of water adsorption on Na–Montmorillonite/New data owing to the use of a continous procedure, in: A.T. Liapis (Ed.), Fundamentals of Adsorption, A.I. Ch. E., New York, 1987, pp. 473–482.
[23] L. Simoni, B.A. Schrefler, An accelerated algorithm for parameter identification in a hierarchical plasticity model accounting for material constraints, Int. J. Numer. Anal. Methods Geomech. 25 (2001) 263–272.
[24] L. Simoni, B.A. Schrefler, Parameter indentification for a suction-dependent plasticity model, Int. J. Numer. Anal. Methods Geomech. 25 (2001) 273–288.
[25] H. Stehfest, Numerical inversion of Laplace transforms, Commun. ASM 13 (1970) 47–49.
[26] G. Swoboda, Y. Ichikawa, Q. Dong, M. Zaki, Back analysis of large geotechnical models, Int. J. Numer. Anal. Methods Geomech. 23 (1999) 1455–1472.
[27] A. Tarantola, Inverse Problem Theory, Elsevier, Amsterdam, 1987.
[28] H.R. Thomas, Y. He, A coupled heat-moisture transfer theory for deformable unsaturated soil and its algorithmic implementation, Int. J. Numer. Methods Eng. 40 (18) (1997) 3421–3441.
[29] H.R. Thomas, Y. He, C. Onofrei, An examination of the validation of a model of the hydro-thermo-mechanical behaviour of engineered clay barriers, Int. J. Numer. Anal. Methods Geomech. 22 (1) (1998) 49–71.
[30] H.R. Thomas, S.W. Rees, N.J. Sloper, Three-dimensional heat, moisture and air transfer in unsaturated soils, Int. J. Numer. Anal. Methods Geomech. 22 (2) (1998) 75–95.
[31] G. Vachaud, M. Vauclin, Comments on a numerical model based on coupled one-dimensional Richards and Boussinesq equations, Water Resour. Res. 11 (3) (1975) 506–509.
[32] G. Vachaud, D. Khanji, M. Vauclin, Experimental and numerical study of a transient two-dimensional unsaturated–saturated water table recharge problem, Water Resour. Res. 15 (5) (1979) 1089–1101.
[33] H.F. Wang, D.J. Hart, Experimental error for permeability and specific storage from pulse decay measurements, Int. J. Rock Mech. Min. Sci. Geomech. Abstr. 30 (7) (1993) 1173–1176.
[34] R.N. Yong, D.M. Xu, A.M.O. Mohamed, An analytical technique for evaluation of coupled heat and mass flow coefficients in unsaturated soil, Int. J. Numer. Anal. Methods Geomech. 16 (1992) 233–246.
[35] M. Zhang, M. Takahashi, R.H. Morin, T. Esaki, Evaluation and application of the transient-pulse technique for determining the hydraulic properties of low-permeability rocks. Part 1: Theoretical evaluation, ASTM Geotech. Testing J. 23 (1) (2000) 83–90.
[36] M. Zhang, M. Takahashi, R.H. Morin, T. Esaki, Evaluation and application of the transient-pulse technique for determining the hydraulic properties of low-permeability rocks. Part 2: Experimental application, ASTM Geotech. Testing J. 23 (1) (2000) 91–99.